16th World Congress in Computational Mechanics (WCCM)
21-26 July 2024, Vancouver, Canada
A. Korobenko, M. Laforest, S. Prudhomme, R. Vaziri (Eds)

INVESTIGATING THE REGION OF ATTRACTION OF SDRE APPLIED TO A CUBESAT ATTITUDE CONTROL SYSTEM DURING THE LAUNCH ORBIT PHASE BASED ON COLD GAS THRUSTERS

ALESSANDRO GERLINGER ROMERO[1] **AND LUIZ CARLOS GADELHA DE SOUZA**[2]

[1] Space Mechanics and Contro Division
National Institute of Space Research
Astronautas Avenue, 1758 - São José dos Campos
BRAZIL
romgerale@yahoo.com.br

[2] Aerospace Engineering Center
Federal University of ABC
Al. da Universidade, s/n - Anchieta - São Bernardo do Campo
BRAZIL
luiz.gadelha@ufabc.edu.br

Key words: SDRE, CubeSat, Cold, Gas, Region, Attraction.

Abstract. The precision of controlling the attitude of a CubeSat during the injection phase in orbit is of fundamental importance for the success of the mission. In general, the CubeSat starts this phase with high angular velocity, and then the controller needs to maneuver the CubeSat to its nominal mode of operation, which is characterized by an attitude of small angles. One way to achieve such a transition between these two modes is by using cold gas thrusters. In this paper, we investigate the region of attraction (ROA) of the State-Dependent Riccati Equation (SDRE) applied to the Attitude Control System (ACS) algorithm during the Launch and Early Orbit Phase which has nonlinear dynamics due to the high angular velocities and perturbations. The SDRE controller is based on cold gas thruster torques to reduce the high angular velocities. The main result of this investigation is the approach to numerically approximate the ROA.

1 INTRODUCTION

Recent years have witnessed a tremendous increase in interest in Cube-Satellites (CubeSats) among the space community including space agencies, industry, and academia. Indeed, the total cumulative launched CubeSats as of August, 1st, 2022 is 2068 including launch failures [1].

The requirements for attitude control of such CubeSats had been evolving in a way that a propulsion subsystem had become common [2, 3]. A propulsion subsystem is the primary mobility device of a spacecraft supporting orbit maneuvers and also attitude control.

The precision of controlling the attitude of a CubeSat during the injection phase in orbit is of fundamental importance for the success of the mission. In fact, in the majority of missions, the launch and early orbit phase (LEOP) is the most critical phase, in which the demand for actuators is the highest [4]. In general, the CubeSat starts this phase with high angular velocities, and then the controller needs to maneuver the CubeSat to its nominal mode of operation, which is characterized by an attitude of small angles. One way to achieve such a transition between these two modes is by using cold gas thrusters [2, 3].

Furthermore, the design of a satellite attitude control subsystem (ACS) that involves plant uncertainties, large angle maneuvers, and fast attitude control following a stringent pointing, requires nonlinear control methods in order to satisfy performance and robustness requirements.

An example is the Nano-satellite Constellation for Environmental Data Collection (CONASAT) [5, 6], a set of remote sensing CubeSats from the Brazilian National Institute for Space Research (INPE), in which the ACS must stabilize the satellite in three-axes in order to maximize the receiving of environment data sent by platforms in the Brazilian territory.

One candidate method for a nonlinear ACS controller is the State-Dependent Riccati Equation (SDRE) method, originally proposed by [7] and then explored in detail by [8, 9, 10]. SDRE provides an effective algorithm for synthesizing nonlinear feedback control by allowing nonlinearities in the system states while offering great design flexibility through state-dependent weighting matrices.

The origin of an SDRE controlled system is a locally asymptotically stable equilibrium point [10]. Furthermore, the knowledge of its region of attraction (ROA) is fundamental due to the local stability even more in the presence of nonlinearities. Indeed, much criticism has been leveled against the SDRE technique since it does not provide assurance of global asymptotic stability. However, empirical experience shows that in many cases the region of attraction may be as large as the domain of interest [8]. Moreover, there are situations in which global asymptotic stability cannot be achieved (for example, systems with multiple equilibrium points). Therefore, especially in aerospace, estimating the region of attraction is fundamental [8].

In this paper, we share an approach to numerically approximate the ROA of CONASAT controlled by SDRE based on cold gas thruster torques to reduce the high angular velocities.

To the best of our knowledge, CONASAT [5, 6] is not planned to have inertial actuators so the evaluation presented here used the available data of the CubeSat augmented with the minimal commonly used thrust to be obtained from a propulsion subsystem based on cold gas. Such evaluation is in accordance with a trend in the CubeSat industry [3, 2], to use inertial actuators for LEOP and orbital maneuvers.

The investigation through a Monte Carlo perturbation model numerically approximates the ROA of the SDRE controller.

2 PROBLEM DESCRIPTION

The SDRE technique entails factorization (that is, parametrization) of the nonlinear dynamics into the state vector and the product of a matrix-valued function that depends on the state itself. In doing so, SDRE brings the nonlinear system to a (nonunique) linear structure having

SDC matrices given by Eq. (1).

$$\begin{aligned}\dot{\vec{x}} &= A(\vec{x})\vec{x} + B(\vec{x})\vec{u} \\ \vec{y} &= C\vec{x}\end{aligned} \tag{1}$$

where $\vec{x} \in \mathbb{R}^n$ is the state vector and $\vec{u} \in \mathbb{R}^m$ is the control vector. Notice that the SDC form has the same structure as a linear system, but with the system matrices, A and B, being functions of the state vector. The nonuniqueness of the SDC matrices creates extra degrees of freedom, which can be used to enhance controller performance, however, it poses challenges since not all SDC matrices fulfill the SDRE requirements, e.g., the pair (A,B) must be pointwise stabilizable.

The system model in Eq. (1) is subject of the cost functional described in Eq. (2).

$$J(\vec{x_0}, \vec{u}) = \frac{1}{2}\int_0^\infty (\vec{x}^T Q(\vec{x})\vec{x} + \vec{u}^T R(\vec{x})\vec{u})dt \tag{2}$$

where $Q(\vec{x}) \in \mathbb{R}^{n\times n}$ and $R(\vec{x}) \in \mathbb{R}^{m\times m}$ are the state-dependent weighting matrices. In order to ensure local stability, $Q(\vec{x})$ is required to be positive semi-definite for all $\vec{x}$ and $R(\vec{x})$ is required to be positive for all $\vec{x}$.

The SDRE controller linearizes the plant about the current operating point and creates constant statespace matrices so that the LQR can be used. This process is repeated in all sampling steps, resulting in a pointwise linear model from a non-linear model, so that an algebraic Riccati equation (ARE) is solved and a control law is computed also in each step. Therefore, according to LQR theory and Eq. (1) and (2), the state-feedback control law in each sampling step is $\vec{u} = -K(\vec{x})\vec{x}$ and the state-dependent gain $K(\vec{x})$ is obtained by Eq. (3) [9].

$$K(\vec{x}) = R^{-1}(\vec{x})B^T(\vec{x})P(\vec{x}) \tag{3}$$

where $P(\vec{x})$ is the unique, symmetric, positive-definite solution of the algebraic state-dependent Riccati equation (SDRE) given by Eq. (4) [9].

$$\begin{aligned} P(\vec{x})A(\vec{x}) + A^T(\vec{x})P(\vec{x}) \\ -P(\vec{x})B(\vec{x})R^{-1}(\vec{x})B^T(\vec{x})P(\vec{x}) \\ +Q(\vec{x}) = 0 \end{aligned} \tag{4}$$

Considering that Eq. (4) is solved in each sampling step, it is reduced to an ARE.

2.1 Region of Attraction

One is frequently interested in the region of attraction (ROA; also called the domain of attraction or the basin of attraction), i.e., the region of the statespace in which the initial conditions of the trajectories lie in order to attain stable behavior [11].

Equilibrium points, if exist, must lie in the regions of attraction, indeed, a state $x_e \in \mathcal{R}^n$ is an equilibrium point of a nonlinear dynamical system $\dot{x} = f(x)$ if $x_0 = x_e \implies x(t) = x_e, \forall\, t > 0$ so $f(x_e) = 0$. A nonlinear system can have an infinite number of equilibrium points, and, each one can be stable or unstable.

Such equilibrium points, if exist, lie in the regions of attraction, which are defined by their attractors. An attractor is a subset $A \in \mathcal{R}^n$ of the statespace characterized by the following three conditions: (i) $a \in A \implies f(a,t) \in A, \forall\, t > 0$; (ii) there exists a vicinity of A (region of attraction) which consists of all trajectories that enter A for $t \to \infty$; and, (iii) there is no proper (non-empty) subset of A having the first two properties. The attractors can be classified into: (I) Fixed point - the final state that a dynamic system evolves towards corresponds to an attracting fixed point, i.e., stable equilibrium point; (II) Limit cycle - a periodic orbit; (III) Quasiperiodic - it exhibits irregular periodicity; (IV) Strange attractor - when such sets cannot be easily described.

Regarding the fixed point attractor, it can be defined by the following equation [12].

$$A = \{x_0 \in \mathcal{R}^n : \lim_{t \to +\infty} x(t, x_0) = 0\} \tag{5}$$

It is important for practical reasons to have information about the size and/or the shape of A. Indeed, the stability properties could be of scarce utility if the region of attraction is very small, or if the equilibrium point is very close to its boundary.

3 SATELLITE PHYSICAL MODELING

This paper is focused on the Launch and Early Orbit Phase (LEOP) of the CONASAT [5, 6], a CubeSat configured in an 8U structure in the Table 1.

3.1 Propulsion Subsystem

The simplest cold gas propulsion subsystem is roughly composed of a cold gas propellant tank and the thrusters controlled by solenoid valves. The simplified operation principle is as follows: (A) the propellant tank is filled with a highly pressurized gas propellant; and (B) the gas flow is controlled by the solenoid valves before the thrusters; (C) once the solenoid valves are activated, high pressurized propellant gas is expanded and accelerated through the nozzle, obtaining the desired thrust [3].

The minimalist design of such propulsion subsystems has a lower mass, a lower power requirement and a higher robustness. Nonetheless, the tank pressure decreases throughout the mission due to the use of the propellant stored in the tank, and, consequently, the maximum thrust produced by the subsystem decreases [3].

The cold gas propulsion subsystem, available in the simulator, is modeled by three thruster pairs, one for each rotation: yaw, pitch and roll. The thrusters of a pair are mounted in the opposite faces of the satellite so they are 0.1 meters from the respective principal axis of inertia of the satellite, moreover, they are positioned back to back so that the nozzles are able to generate

Table 1: Satellite characteristics and references.

Name	Value
Satellite Characteristics [5, 6]	
unit	8U
size (m)	$\begin{bmatrix} 0.2 & 0.2 & 0.2 \end{bmatrix}^T$
mass (kg)	8.2
inertia tensor ($kg.m^2$)	$\begin{bmatrix} 0.0547 & 0 & 0 \\ 0 & 0.0519 & 0 \\ 0 & 0 & 0.0574 \end{bmatrix}$
Actuators Characteristics - Thrusters	
maximum thrust (mN)	10
References for the controller	
Sun versor in the body (XYZ)	$\begin{bmatrix} 1 & 0 & 0 \end{bmatrix}^T$
angular velocity ($radians/second$, XYZ)	$\begin{bmatrix} 0 & 0 & 0 \end{bmatrix}^T$

symmetric torques. Hence, the external torque is defined by Eq. (6).

$$\vec{g_{cm}} = -\sum_{n=1}^{3} \vec{r_n} \times T_n \vec{a_n} \vec{a_n}^T \tag{6}$$

where g_{cm} is the external torque obtained in the centre of mass of the satellite, T_n is the magnitude of the thrust obtained in the symmetry axis $\vec{a_n}$ by each pair of opposite nozzles, and r_n is the position vector, which is a vector from the centre of mass of the satellite about which the torque is being computed to the symmetry axis $\vec{a_n}$ of the nozzles.

Recall due to the nature of solenoids, the type of control of such a propulsion subsystem is an ON-OFF, which leads to an impulsive control [13].

3.2 Kinematics

Given the ECI reference frame ($\mathfrak{F}_i$) and the frame defined in the satellite with origin in its centre of mass (the body-fixed frame, $\mathfrak{F}_b$), then a rotation $R \in SO(3)$ represented by an unit quaternion $Q = [q_1 \; q_2 \; q_3 \mid q_4]^T$ can define the attitude of the satellite. Recall $SO(3)$ is the set of all attitudes of a rigid body described by 3×3 orthogonal matrices whose determinant is one.

Defining the angular velocity $\vec{\omega} = [\omega_1 \, \omega_2 \, \omega_3]^T$ of $\mathfrak{F}_b$ with respect to $\mathfrak{F}_i$ measured in the $\mathfrak{F}_b$, the kinematics can be described by Eq. (7) [14].

$$\dot{Q} = \frac{1}{2}\Omega(\vec{\omega})Q = \frac{1}{2}\Xi(Q)\vec{\omega}$$

$$\Omega(\vec{\omega}) \triangleq \begin{bmatrix} 0 & \omega_3 & -\omega_2 & \omega_1 \\ -\omega_3 & 0 & \omega_1 & \omega_2 \\ \omega_2 & -\omega_1 & 0 & \omega_3 \\ -\omega_1 & -\omega_2 & -\omega_3 & 0 \end{bmatrix}, \tag{7}$$

where the unit quaternion Q satisfies the following identity:

$$q_1^2 + q_2^2 + q_3^2 + q_4^2 = 1 \tag{8}$$

Eq. (7) allows the prediction of the satellite's attitude if it is available the initial attitude and the history of the change in the angular velocity ($\dot{Q} = F(\omega, t)$).

Another possible derivation of the Eq. (7) is using the vector g (Gibbs vector or Rodrigues parameter) as $Q = [g^T|q_4]$.

$$\dot{Q} = -\frac{1}{2}\begin{bmatrix}\omega^{\times} \\ \omega^T\end{bmatrix}\begin{bmatrix}q_1 \\ q_2 \\ q_3\end{bmatrix} + \frac{1}{2}q_4\begin{bmatrix}1_{3\times3} \\ 0\end{bmatrix}\omega\,, \tag{9}$$

where $\omega^{\times}$ is the cross-product skew-symetric matrix of $\vec{\omega}$ and 1 is the identity matrix.

3.3 Rotational Dynamics

In order to know the history of the change in the angular velocity, it is necessary to understand the history of the change in the angular acceleration ($\dot{\vec{\omega}} = G(\tau, t)$) of the satellite. According to the Euler-Newton formulation of the rotational motion, angular acceleration is caused by torques, in other words, the change in the angular momentum $\dot{\vec{h}}$ is equal to the net torques $\vec{g}$ applied in the satellite, see Eq. (10) (the present subsection is derived based on the centre of mass of the satellite, for the general case, see [14]).

$$\dot{\vec{h}} = \vec{g} \tag{10}$$

Taking into account the motion of the body-fixed frame $\mathfrak{F}_b$ with respect to the ECI $\mathfrak{F}_i$ and the angular velocity $\vec{\omega}$, the derivative of the angular momentum in $\mathfrak{F}_b$ is defined by Eq. (11).

$$\dot{\vec{h}} = \vec{g} - \vec{\omega} \times \vec{h} \tag{11}$$

Furthermore, $\dot{\vec{h}} = I.\dot{\vec{\omega}}$ and $\vec{h} = I.\vec{\omega}$, where I is the time-invariant inertia tensor. The combination of this definition and Eq. (11) results in Eq. (12).

$$I.\dot{\vec{\omega}} = \vec{g} - \vec{\omega} \times (I.\vec{\omega}) \tag{12}$$

Recall the satellite has three thruster pairs, each pair aligned with the principal axes of inertia of the satellite, moreover, such type of actuator, inertial actuators, generates external torques.

Therefore, the motion of the satellite is described by Eq. (13) .

$$\dot{\omega} = I^{-1} g_{cm} - I^{-1} \omega^{\times} I \omega \, , \tag{13}$$

where g_{cm} is the external torque produced by the thrusters.

4 CONTROLLER DESIGN AND REGION OF ATTRACTION

Two dynamics states must be controlled: (1) the attitude (modeled as unit quaternions Q by Eq. (7) or Eq. (9)) and (2) its stability ($\dot{Q}$, in other words, the angular velocity ω of the satellite by Eq. (13)). The following subsections explore the state-space modeling, the synthesis of controller and the region of attraction.

4.1 Nonlinear Control based on SDRE

Assuming that the net external torques (g_{cm}) are solely defined by the thrusters, the rotational dynamics is defined in Eq. (13).

Choosing state as $x_1 = Q$ and $x_2 = \omega$, and the control vector as $u_1 = T_c = g_{cm}$, then the state space model can be defined using Eq. (9) and (13), which leads to Eq. (14).

$$\begin{gathered}
\begin{bmatrix} \dot{x_1} \\ \dot{x_2} \end{bmatrix} = \begin{bmatrix} -\frac{1}{2} \begin{bmatrix} \omega^{\times} \\ \omega^{T} \end{bmatrix} & 0 & \begin{bmatrix} \frac{1}{2} q_4 1_{3\times3} \\ 0 \end{bmatrix} \\ 0 & 0 & -I^{-1}\omega^{\times} I \end{bmatrix} \begin{bmatrix} x_1 \\ x_2 \end{bmatrix} + \begin{bmatrix} 0 \\ I^{-1} \end{bmatrix} \begin{bmatrix} u_1 \end{bmatrix} \\
\begin{bmatrix} y \end{bmatrix} = 1_{1\times7} \begin{bmatrix} x_1 \\ x_2 \end{bmatrix}
\end{gathered} \tag{14}$$

Eq. (14) has been shown to satisfy SDRE conditions in the majority of statespace except for the region on which the angular velocities are close to 0 (the pair(A,B) loses rank in such region). Note this known limitation of this particular parametrization of SDRE imposes laxity.

4.2 Region of Attraction

Firstly, the control law is modeled and too many time-domain simulations are available for analysis. Therefore, the main task is to assess the presence of a fixed point attractor as well as its size and shape.

Nonetheless, it is somewhat difficult to depict the ROA for statespace systems with dimensions higher than three.

Inspired by the works of Henri Poincaré, in particular, Poincaré maps [15] which defines a lower-dimensional subspace for qualitative analysis. The present paper applied two Euclidean norms, namely L2-norm of Euler angles and L2-norm of angular velocities, to define a two-dimensional space for qualitative and quantitative analysis. In such a way that the area of the ROA (dimensionless quantity) can be analytically computed; and, the plot of the ROA can allow straightforward qualitative analysis.

Besides, the definition of the fixed point attractor presented in Equation (5) is restricted by the accounting of an explicit final time t_f and a numerical error ϵ, according to the following equation:

$$A = \{x_0 \in \mathcal{R}^n : \lim_{t \to t_f} ||x(t, x_0)||_2 < \epsilon\} \tag{15}$$

Equipped with (A) the two-dimensional space for qualitative analysis of the original seven-dimensional statespace, and (B) Equation (15), simple polygons (they do not intersect themselves and have no holes) of ROAs are defined in the two-dimensional space for the initial conditions x_0.

Taking into account the limitations of the control laws previously stated in Subsection 4.1, the definition of the fixed point attractor presented in Equation (15) is once restricted by the selection of sole angular velocities (x_2 in Equation (14)), ω-stability in [14], according to the following equation:

$$A = \{x_0 \in \mathcal{R}^n : \lim_{t \to t_f} ||x_2(t, x_0)||_2 < \epsilon\} \tag{16}$$

Focusing on the area of ROAs A, one defines a Monte Carlo perturbation model for a given set of initial conditions, performs the time-domain simulation until the predefined t_f, and, finally, computes such a measure.

5 SIMULATION RESULTS

The results were computed using the satellite (modeled as a nonlinear system) and the control law (SDRE). Furthermore, such results were obtained running a full Monte Carlo perturbation model described as follows.

Regarding initial attitudes defined by 3-2-1 Euler angles (Z-Y-X, nonclassical Euler angles), it is well-known that representing Y beyond ± 90 degrees (that means ± 180 degrees) would give two Euler angles solution for every rotation, so Y is limited to ± 90 degrees. X and Z are limited to ± 180 degrees. Therefore, independent distributions are applied for each Euler angle respecting the limits previously discussed in order to define the initial attitudes (3-2-1, Z-Y-X, nonclassical Euler angles, which are converted in quaternions) in a given Monte Carlo perturbation model.

Regarding initial angular velocities, they are defined by independent distributions based on a limit.

In summary, the approach for the evaluation of the region of attraction can be summarized as:

- Compute initial conditions for the Monte Carlo perturbation model

  Using independent distributions, compute the 3-2-1 Euler angles (Z-Y-X, nonclassical Euler angles) in the range $(\pm 180, \pm 90, \pm 180)$

  Using independent distributions, compute the angular velocities

Table 2: Monte Carlo perturbation model parameters.

Name	Value
3-2-1 Euler angles (degrees)	$Z : U(-180, 180)$ $Y : U(-90, 90)$ $X : U(-180, 180)$
angular velocities (rad/s)	$X : U(-0.09, 0.09)$ $Y : U(-0.09, 0.09)$ $Z : U(-0.09, 0.09)$
Q	I
R	I
ϵ (rad/s)	0.01
samples	200
t_f (seconds)	1000
fixed step size (seconds)	0.1

- Perform the time-domain simulation until the predefined t_f
- Compute ROA

The results are based on the satellite CONASAT, which is characterized by Table 1, furthermore, the simulations were conducted with the full Monte Carlo perturbation model tuned with the parameters shared in Table 2.

The initial conditions uniformly distributed computed using such parameters by the Monte Carlo perturbation model are depicted using a two-dimensional space, in which the norm of Euler angles is along the X-axis and the norm of angular velocities is along the Y-axis for each initial condition. This space has its bounds constrained by the norm of Euler Angles ranging from 0 to 270 degrees and the norm of angular velocities ranging from 0 to approximately 0.15 radians per second, following the parameters presented in Table 2. The same two-dimensional space is used to depict ROAs.

Figure 1 shows the initial conditions uniformly distributed by such a Monte Carlo perturbation model execution.

The result of the Monte Carlo perturbation model execution is depicted in Figure 2 which shows the ROA of SDRE for CONASAT for the computed initial conditions.

6 CONCLUSION

As the results are based on analysis through simulations, they are neither valid for general cases nor scenarios out of the range of the Monte Carlo perturbation models due to the underlying nonlinear dynamics.

Although the results numerically approximate the ROA of SDRE in the case of CONASAT, the major contribution of the paper is the approach for the evaluation of the ROAs since the

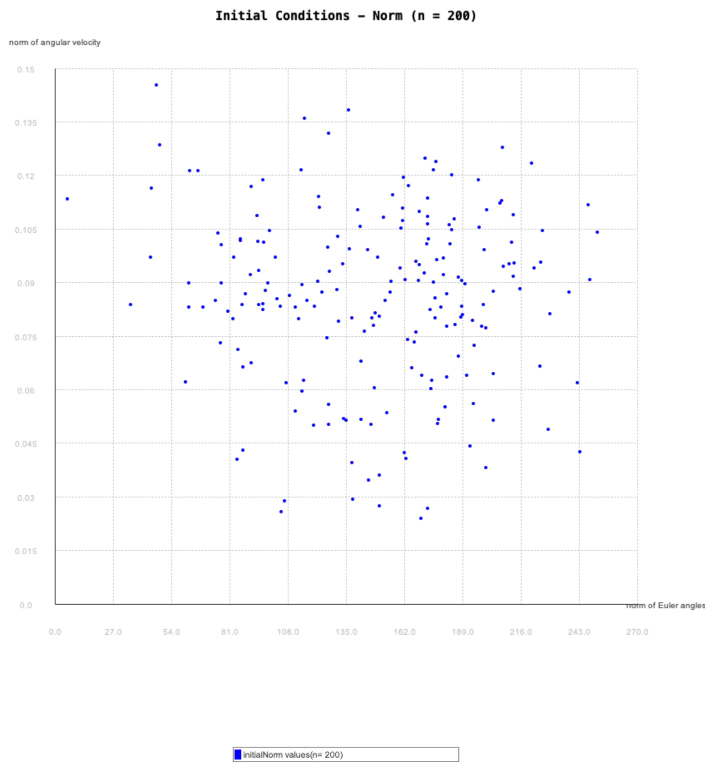

Figure 1: Initial conditions.

approach provides a tractable numerical algorithm to compare control techniques. Moreover, confidence turns out to be a matter of computational power.

REFERENCES

[1] Erik Kulu. *Nanosatellite Launch Forecasts 2022: Track Record and Latest Prediction*. Proceedings of the 36th Annual Small Satellite Conference, (2022).

[2] Tummala, Akshay Reddy and Dutta, Atri. *An Overview of Cube-Satellite Propulsion Technologies and Trends*. Journal of Aerospace, Vol. 4, Number 4, ISSN 2226-4310, (2017).

[3] Kristina Lemmer. *Propulsion for CubeSats*. Journal Acta Astronautica, Vol. 134, ISSN 0094-5765, (2017).

[4] Wertz, James R. and Larson, Wiley. *Space mission analysis and design*. Microcosm, (1999).

[5] Manoel Jozeane Mafra de Carvalho. *Estudo de uma Missão Espacial para Coleta de Dados Ambientais Baseada em Nano Satélites*. Inpe, (2010).

[6] B. D. Reis de Mesquita and H. Koiti Kuga and V. Carrara. *Estimation and Attitude Control in CONASAT Nominal Operation Mode: An Approach for SDRE Filter and PID Control*. IEEE Latin America Transactions, Vol. 15, Number 5, (2017).

[7] Pearson, J. D. *Approximation methods in optimal control i. sub-optimal control*. Journal of Electronics and Control, Vol. 13, Number 5, (1962).

[8] Çimen, Tayfun. *Asymptotic stabilization,Nonlinear system control,Optimal control theory*. IFAC Proceedings Volumes (IFAC-PapersOnline), Vol. 17, Number 1, (2008).

[9] Çimen, Tayfun. *Systematic and effective design of nonlinear feedback controllers via the state-dependent Riccati equation (SDRE) method*. Annual Reviews in Control, Vol. 34, Number 1, (2010).

[10] Cloutier, James R and D'Souza, Christopher N and Mracek, Curtis P. *Nonlinear regulation and nonlinear H-infinity control via the state-dependent Riccati equation technique*. Conference on Nonlinear Problems in Aviation, (1996).

[11] Parks, P. C. and Hahn, V. *Stability Theory*. New York: Prentice-Hall, (1992).

[12] Bacciotti, A.; Rosier, L. *Liapunov functions and stability in control theory*. Springer, (2005).

[13] Tao Yang. *Practical Stability of Impulsive Control*. Impulsive Control Theory, Springer, (2001).

[14] Hughes, Peter C. *Spacecraft attitude dynamics*. New York, (1986).

[15] Leipholz, H. *Stability theory: an introduction to the stability of dynamic systems and rigid bodies*. Academic Press, (1970).

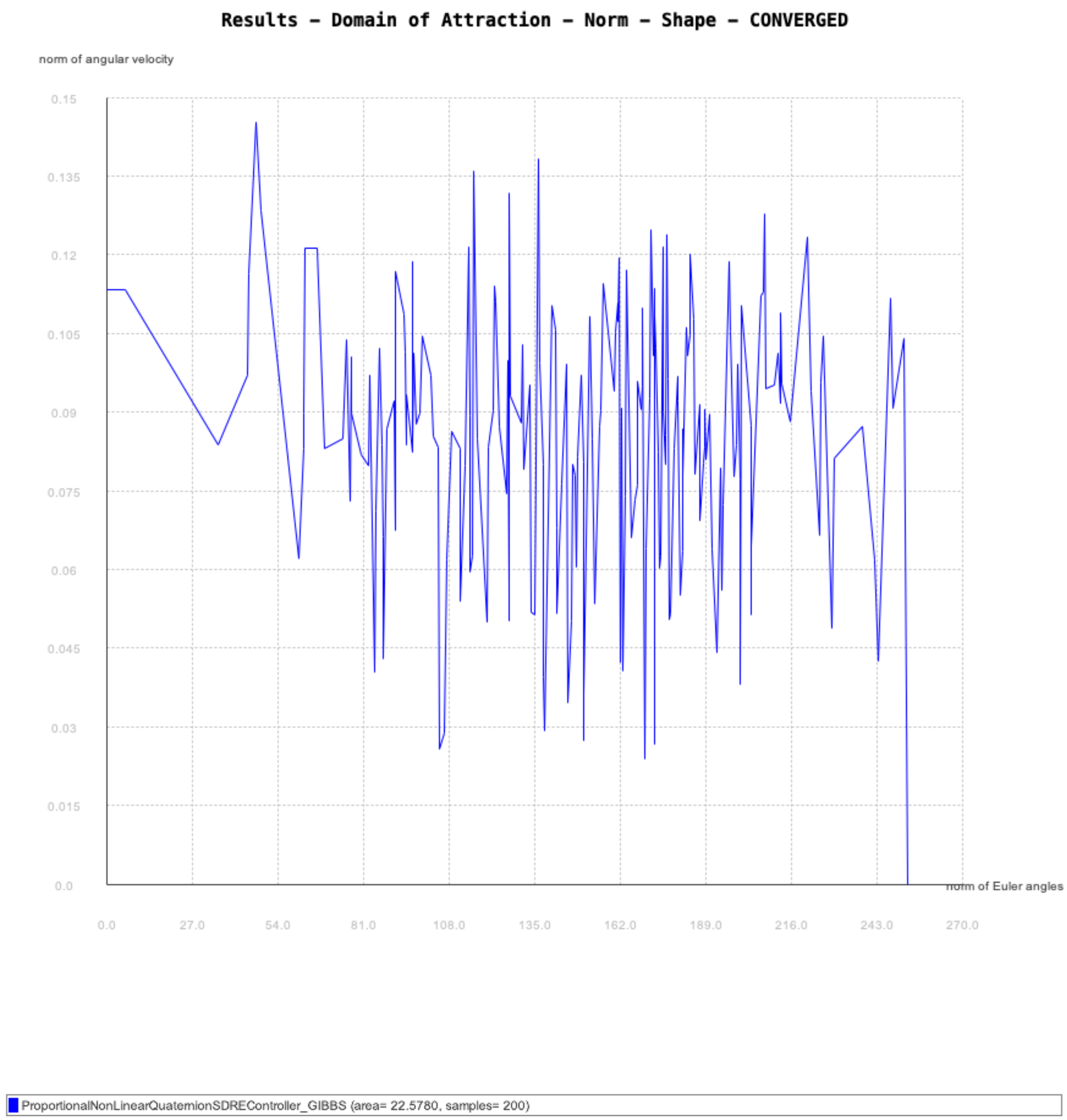
Results - Domain of Attraction - Norm - Shape - CONVERGED
norm of angular velocity
0.15
0.135
0.12
0.105
0.09
0.075
0.06
0.045
0.03
0.015
0.0
norm of Euler angles
0.0
27.0
54.0
81.0
108.0
135.0
162.0
189.0
216.0
243.0
270.0
ProportionalNonLinearQuaternionSDREController_GIBBS (area= 22.5780, samples= 200)

Figure 2: ROA.